Brain Imaging and Behavior (2019) 13:200–209
DOI 10.1007/s11682-017-9765-0

ORIGINAL RESEARCH

Cognitive performance in mid-stage Parkinson's disease: functional connectivity under chronic antiparkinson treatment

Roxana Vancea[1] · Kristina Simonyan[1,2] · Maria Petracca[1,3] · Miroslaw Brys[4] · Alessandro Di Rocco[4] · Maria Felice Ghilardi[5] · Matilde Inglese[1,6,7,8]

Published online: 23 September 2017

Abstract Cognitive impairment in Parkinson's disease (PD) is related to the reorganization of brain topology. Although drug challenge studies have proven how levodopa treatment can modulate functional connectivity in brain circuits, the role of chronic dopaminergic therapy on cognitive status and functional connectivity has never been investigated. We sought to characterize brain functional topology in mid-stage PD patients under chronic antiparkinson treatment and explore the presence of correlation between reorganization of brain architecture and specific cognitive deficits. We explored networks topology and functional connectivity in 16 patients with PD and 16 matched controls through a graph theoretical analysis of resting state-functional MRI data, and evaluated the relationships between network metrics and cognitive performance. PD patients showed a preserved small-world network topology but a lower clustering coefficient in comparison with healthy controls. Locally, PD patients showed lower degree of connectivity and local efficiency in many hubs corresponding to functionally relevant areas. Four disconnected subnetworks were also identified in regions responsible for executive control, sensorymotor control and planning, motor coordination and visual elaboration. Executive functions and information processing speed were directly correlated with degree of connectivity and local efficiency in frontal, parietal and occipital areas. While functional reorganization appears in both motor and cognitive areas, the clinical expression of network imbalance seems to be partially compensated by the chronic levodopa

✉ Matilde Inglese
matilde.inglese@mssm.edu

Roxana Vancea
roxana.oana@gmail.com

Kristina Simonyan
kristina.simonyan@mssm.edu

Maria Petracca
maria.petracca@mssm.edu

Miroslaw Brys
Miroslaw.Brys@nyumc.org

Alessandro Di Rocco
Alessandro.DiRocco@nyumc.org

Maria Felice Ghilardi
lice.mg79@gmail.com

[1] Department of Neurology, Icahn School of Medicine, Mount Sinai, One Gustave L. Levy Place Box 1137, New York, NY 10029, USA

[2] Annenberg Building Floor 20 Room 82, 1468 Madison Avenue, New York, NY 10029, USA

[3] Department of Neuroscience, Universita' "Federico II", Napoli, Italy

[4] Department of Neurology, New York University School of Medicine, NYU Movement Disorders, 240 East 38th Street, 20th Floor, New York, NY 10016, USA

[5] Department of Physiology and Pharmacology, City University of New York Medical School, 138th and Convent Ave, New York, NY 10031, USA

[6] Department of Radiology, Icahn School of Medicine, Mount Sinai, New York, NY, USA

[7] Department of Neuroscience, Icahn School of Medicine, Mount Sinai, New York, NY, USA

[8] Department of Neuroscience, Rehabilitation, Ophthalmology, Genetics, Maternal and Child Health, University of Genova and IRCCS AOU San Martino-IST, Genova, Italy

treatment with regards to the motor but not to the cognitive performance. In a context of reduced network segregation, the presence of higher local efficiency in hubs regions correlates with a better cognitive performance.

Keywords Functional connectivity · Cognition · Parkinson's disease · Graph theory

Introduction

The development of cognitive deficits in Parkinson's disease (PD), predominantly affecting working memory, attentional processes and response inhibition, is related to the disruption of cortico-cerebellar loops, cholinergic circuits and dopamine signaling to the prefrontal cortex (Matsumoto 2015).

In order to investigate neural networks integration in PD, several studies have explored brain's topological organization through graph theory (Göttlich et al. 2013; Lebedev et al. 2014; Luo et al. 2014; Sang et al. 2015; Skidmore et al. 2011; Zhang et al. 2014), which allows the assessment of local and global connectivity between brain networks, mathematically represented as a set of nodes (i.e. brain regions) connected by edges (Bullmore et al. 2009). So far, graph theory studies in PD have mainly disclosed the presence of a disconnection syndrome, characterized by lower degree of processing efficiency at both local and global level (Luo et al. 2015; Sang et al. 2015).

Among these studies, only two have investigated the relationship between brain functional reorganization and cognitive status, both focusing on drug-naïve patients (Lebedev et al. 2014; Luo et al. 2015). While the role of prolonged chronic therapy with dopaminergic drugs on the cognitive status of PD patients is still controversial (Poletti and Bonuccelli 2013), it is known from drug challenge studies that levodopa treatment can modulate metabolic response and enhance functional connectivity in motor and cognitive brain circuits (Esposito et al. 2013; Mattis et al. 2011). This raises the question of which changes in brain topology might derive from the concurrent impact of PD pathological processes and use of prolonged antiparkinson treatment. Therefore we sought to use graph theoretical analysis to characterize brain topology of mid-stage PD patients under chronic antiparkinson treatment and to explore the presence of correlations between reorganization of brain architecture and cognitive deficits.

Materials and methods

Subjects

Sixteen patients (8 males/8 females; age 62.25 ± 8.64 years, disease duration 10.02 ± 4.50) with clinically diagnosed idiopathic PD according to the clinical diagnostic criteria of the United Kingdom Parkinson's Disease Society Brain Bank (Hughes et al. 1992), and sixteen age and gender matched healthy subjects (8 males/8 females; age 62.81 ± 7.08 years) were enrolled prospectively from the Parkinson's and Movement Disorders Center of the New York University Langone Medical Center (NYULMC).

Inclusion criteria were (1) age of 45 or older; (2) Hoehn & Yahr stage equal or less than 3 while in an "on" state; (3) disease duration less than 20 years; (4) anti-parkinsonian treatment at a stable and optimized daily dosage for at least 4 weeks prior to study entry. Exclusion criteria were (1) dementia according to clinical examination and the modified Mini Mental State Examination (MMSE); (2) major depression according to DSM-IV criteria for current major depression; (3) clinically significant or unstable medical condition, including serious cardiovascular or cerebrovascular disease; (4) ongoing antidepressant or neuroleptic treatment.

Patients were evaluated 60 to 90 min after their morning dose of levodopa and disease severity was assessed using the Hoehn & Yahr stages and Unified Parkinson's Disease Rating Scale (UPRDS). The mean levodopa equivalent daily dose (LEDD) was 963.53 ± 629.59 mg. PD patients were rated on the UPDRS (Goetz et al. 2007) on a range from 4 to 37 (mean value ± SD 18.12 ± 8.89, range 4–37) and on Hoehn & Yahr staging scale on a range from 1 to 3 (mean value ± SD 1.93 ± 0.68, range 1–3) while on their medication. The MMSE score in PD patients was 28.54 ± 1.63, with a level of education of 15.23 ± 3.19 years.

Clinical and neurological examinations in healthy volunteers were normal and none of them had any history of neurological disease. All participants had normal MRI structural images.

The study was approved by the NYULMC Internal Review Board and all the subjects gave informed written consent prior to participation.

Neuropsychological evaluation

All PD patients underwent neuropsychological evaluation on the same day of the clinical examination, including the following tests: (1) Digit Span Forward (DF) and Backward (DB) to assess attention and working memory; (2) Digit Symbol Substitution (DSS) to assess processing speed; (3) California Verbal Learning Test (CVLT) to assess verbal memory; (4) Wisconsin Card Sorting Test (WCST) to assess executive functions; (5) Delis-Kaplan Executive Function System Trail Making Test (TMT) to assess visual attention and task switching. In addition, the Hamilton Depression Rating Scale was administered to evaluate the presence and severity of slow mood, insomnia, agitation and anxiety. Raw scores for neuropsychological tests are reported in Table 1.

Functional magnetic resonance imaging

All subjects underwent an MRI scan on a 3T scanner (Tim trio Siemens Medical Solutions, Enlargen, Germany) using the vendor-provided 12-channel phased-array head coil on the same day of the clinical examination. The MRI protocol included: (a) T2 sequence (TR/TE = 5120/90 ms; field of view = 237 × 239 mm^2; matrix = 444 × 448; 55 slices; slice thickness = 2.5 mm; in-plane spatial resolution = 0.56 × 0.56 mm^2); (b) three dimensional (3D) T1 MP-RAGE sequence (TR/TE = 2300/2.98 ms; TI = 900 ms; voxel size = 1 mm isotropic); (c) echo-planar imaging-based sequence (EPI) for resting state fMRI (TR/TE = 2000/30 ms; field of view = 205 × 205 mm^2; matrix = 64 × 64; 35 slices; slice thickness = 3.5 mm; in-plane spatial resolution = 3.2 × 3.2 mm^2).

Resting state-functional MRI image post-processing

Functional images were processed and analyzed by using Analysis of Functional NeuroImage (AFNI) software (https://afni.nimh.nih.gov). The hardware-related noise in the time series was regressed out based on the anatomy-based correlation corrections (ANATICOR) model; including motion parameters, local white matter and ventricles as regressors. The resulting images were smoothed and normalized and the final step of the pre-processing workflow included alignment to the Talairach space (TT_N27 standard). Brain segmentation into 206 regions of interest was performed in the MNI 152 space using the Eickhoff-Zilles probabilistic atlas within AFNI. For the construction of functional brain networks, the level of functional connectivity between each pair of regions of interest in the network was computed for each data set as the correlation between their averaged regional time series by using Pearson's correlation coefficient in Matlab (v 7.12). For the graph construction, these correlation coefficients represented the weights of the graph's edges, and the regions of interest constituted the nodes ($N = 206$) for every subject's brain network. The result of the pre-processing stage was a static, fully-connected, weighted, undirected, connectivity matrix for each subject.

Table 1 Raw scores for NPS battery in PD patients

Digit span forward	10.13 ± 2.36
Digit span backward	6.93 ± 2.05
Digit symbol substitution	52.67 ± 12.51
California verbal learning test-total correct	28.47 ± 3.83
California verbal learning test-short delay free recall	7.73 ± 1.28
California verbal learning test-long delay free recall	7.40 ± 1.88
Wisconsin card sorting test- total correct	47.67 ± 7.43
Trail making test- visual scanning	31.93 ± 11.52
Trail making test- number sequencing	57.07 ± 26.32
Trail making test- letter sequencing	48.27 ± 22.63
Trail making test- motor speed	36.87 ± 16.67
Hamilton depression rating scale	6.60 ± 3.98

All values are expressed as mean ± SD

Graph theory analysis

The positive correlations from the brain networks, that represent regional activity interaction, were defined by a weighted system as connectivity matrix.

In order to remove 'noisy' connections, the connectivity matrix was thresholded over a range of connection densities by using 19 sparsity levels with a 5% gap among them. The sparsity levels (κ) represent the supra-threshold connections relative to the total possible connections ($1 < \kappa < 19$). Edges showing a weight less than 10% of the maximum weight in the network were considered noise and therefore removed.

A 206 × 206 connectivity matrix was generated for each of the 19 sparsity levels in each subject. To ensure variance stabilization, the Fisher Z transformation was computed on the correlation matrices. The small-world topology and the inter-regional activity interactions were analyzed with specific graphs parameters in Matlab, using Brain Connectivity Toolbox (https://sites.google.com/a/brain-connectivity-toolbox.net/bct/). We selected graphs metrics of interest in order to assess both regional and global network properties. As global measures we explored characteristic path length (L) that is a measure of communication efficiency within the network, and clustering coefficient (C), which is a measure of the nodes' tendency to group together into tightly connected clusters. As local measures we selected the degree of connectivity (D), which reflects the degree of interaction of each node with all the other nodes in the network and the local efficiency (E_l) that expresses the level of communication between neighboring nodes. While L and C characterize the overall structure of the network, D and E_l allow the exploration of short and long-distance communication integrity.

First, the small-world network properties were evaluated on both groups of subjects using the small-worldness coefficient (σ). A small-world network is characterized by small normalized path length ($\lambda < 1$) and high normalized clustering coefficient ($\gamma >> 1$), defining the small-worldness coefficient as $\sigma = \gamma/\lambda$ (Rubinov and Sporns 2010). In order to compute σ we estimated L, and C. L is estimated evaluating the number of vertices traversed to get information from a source- to a destination- node; a shorter L corresponds to a more integrated network (Worbe et al. 2012). C represents the fraction of a node's neighbors that are also neighbors among them and defines the triangular formations in the graph among three different brain regions that communicate among them, determining clusters. C

and L were normalized using random generated networks ($n = 100$), which were matched to the real ones, preserving the number of nodes and edges. The same sparsity levels (κ) were applied to the random matrices. The C and L obtained from the random graph (L_random, C_random) determined the small-world network parameters (L/L_random = λ ; C/C_random = γ).

Second, D and E_l were computed in both patients and controls. D reflects the number of nodes that communicate with the evaluated one and it is computed as the number of incident edges in that specific node. Nodes with a high D functionally interact with many other nodes in the network (Bullmore et al. 2009). E_l represents the level of communication between neighboring nodes. It reflects the average efficiency of local clusters and thus it defines the fault tolerance of the network (Reijmer et al. 2013).

We also analyzed hub formation in the networks, defining a hub as node in which the value of the parameter of choice was at least one standard deviation greater than the average mean parameter (Bassett and Bullmore 2006). The formation of hubs was examined for both.

Statistical analysis

The statistical analysis was performed with SPSS 19.0 (SPSS INC., Chicago, IL). All graph measures and clinical parameters retained the null-hypothesis when tested with Kruskal–Wallis test for equal distribution within groups. Between-group comparisons on the graph parameters were explored by using a two-tailed t-test for independent samples. Once significant between-group differences in network metrics were observed, we further assessed the relationships between graph parameters and clinical scores by using Spearman's bivariate correlation test. Raw scores of cognitive tests were mean centered for statistical analysis. Level of significance was set at $p < 0.05$. Because of the exploratory nature of this study, multiple testing correction was not performed and therefore the reported P-values should be interpreted as descriptive.

Inter regional correlation in BOLD response was compared between groups using the Network-Based Statistics Toolbox, controlling for family-wise error rate with 5000 iterations and applying a threshold at $t = 6.0$ for the connectivity values ($p < 0.05$). The statistical test used in NBS is performed on the sum of all functional connections surviving the critical t-value. Since the extent of the network depends on the selected t-value, we decided to consider a strict (high) threshold in order to avoid the identification of large components as a matter of chance (Zalesky et al. 2010). Relationships between nodal metrics from disconnected sub-networks and clinical parameters were tested with Spearman's bivariate correlation test.

Results

Global network metrics

A small-world network topology was observed in both patients and controls ($\sigma > 1$). Both groups presented a greater-than-random normalized clustering coefficient ($\gamma >> 1$) (mean ± SD γPD: 1.125 ± 0.141; γHC: 1.050 ± 0.052) and a near-random normalized path length ($\lambda \sim 1$) (mean ± SD ΛPD: 1.008 ± 0.004; ΛHC: 0.998 ± 0.019 (Fig. 1). Clustering coefficient was lower in PD (0.278 ± 0.037) as compared to

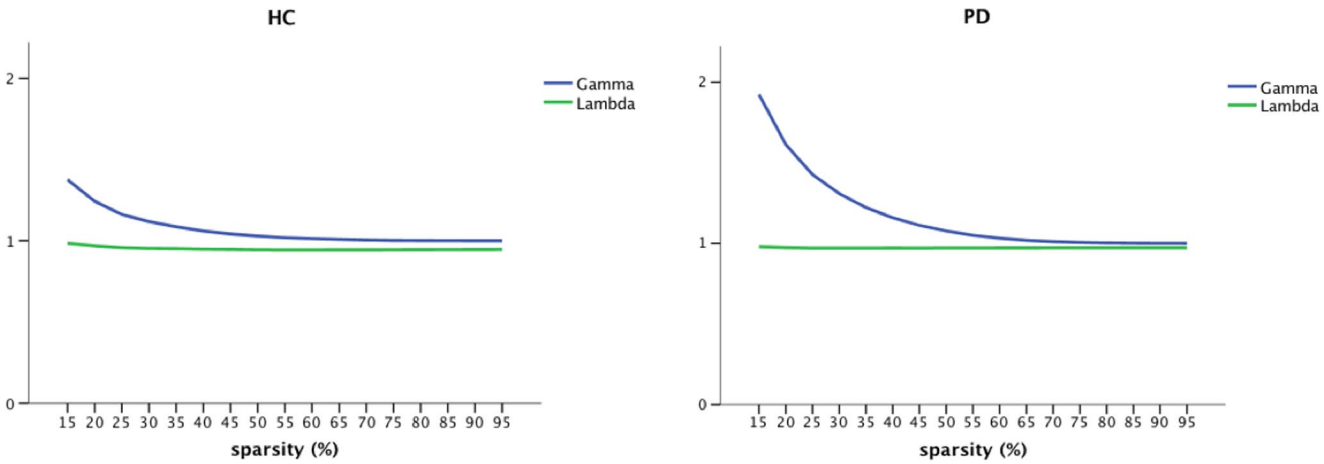

Fig. 1 Small-World Network topology. Normalized clustering coefficient and characteristic path length are shown in the healthy controls (HC) group and in the Parkinson's disease (PD) group as a function of the sparsity. The gamma and lambda were averaged over the networks of each group: HC and PD. At a wide range of sparsity, the networks of each group have an average gamma greater than 1 and an average lambda near to 1, which implies prominent small-world properties

Table 2 Hubs showing a significant lower degree in PD than HC

Brain area	Coordinates			*p*-value
	x	y	z	
Postcentral gyrus, L	−40	−30	52	0.0074 *
Postcentral gyrus, R	46	−27	51	0.0132
Inferior parietal lobule, L	−40	−34	46	0.0149
Inferior frontal gyrus, L	−48	8	31	0.0190
Inferior frontal gyrus, R	49	26	16	0.0082 *
Paracentral lobule, L	−7	−37	58	0.0030 *
Paracentral lobule, R	8	−35	57	0.0006 *
Cuneus, R	14	−74	27	0.0276
Middle occipital gyrus, L	−31	−76	12	0.0022 *
Middle occipital gyrus, R	34	−77	14	0.0026 *
Middle temporal pole, L	−34	13	−26	0.0100
Middle temporal pole, R	42	13	−25	0.0391
Superior parietal lobule, L	−18	−61	52	0.0199
Superior temporal gyrus, L	−61	−20	7	0.0390

Hubs showing a statistically significant lower degree in PD as compared to HC ($p<0.05$). The coordinates are given as stereotaxic coordinates referring to the atlas of Talairach and Tournoux

Abbreviations: L left, *R* right

*$p<0.01$

healthy controls (0.376 ± 0.039), with statistical significantly lower values for PD on a range of sparsity 4–7 ($p<0.05$). Path length was higher in PD (0.997 ± 0.004) than healthy controls (0.989 ± 0.017), but the difference was not statistically significant.

Nodal attributes: degree and local efficiency

Based on their degree of connectivity (D), 23 D hubs were detected in PD and 27 in healthy controls. Among them, 14 hubs showed statistically significant lower degree in PD as compared to healthy controls ($p<0.05$) (Table 2 and Fig. 2a).

Based on local efficiency (E_l), an equal number of hubs ($n=19$) was detected in the two groups. All hubs showed a statistically significant lower E_l in PD than healthy controls ($p<0.05$) (Table 3 and Fig. 2b).

No correlations were detected between UPDRS motor scores and nodal attributes, while some correlations were detected between neuropsychological scores and nodal attributes. DSS was directly correlated with D in the left superior temporal gyrus ($r=0.532$, $p<0.05$) and E_l in the inferior frontal gyrus (left: $r=0.651$, $p<0.01$; right: $r=0.646$, $p<0.01$), supplementary motor area (left: $r=0.730$; $p<0.01$; right: $r=0.687$, $p<0.01$) and left middle occipital gyrus ($r=0.655$, $p<0.01$) while WCST was directly correlated with E_l in the right cuneus ($r=0.534$ $p<0.05$), left inferior parietal lobule ($r=0.537$, $p<0.05$), right post-central gyrus ($r=0.528$, $p<0.05$) and precentral gyrus (left: $r=0.530$, $p<0.05$; right: $r=0.564$, $p<0.05$).

Network based statistic: disconnected sub-networks identification

Analyzing the network topology, we identified four disconnected sub-networks ($p<0.05$) (Table 4 and Figs. 3, 4). The computation of graph theory measures in disconnected sub-networks detected a lower mean value of the local parameters (D, E_l) in PD (Table 5), with the exception of sub-network 1, which includes connection between cerebellum and the anterior cingulate cortex. Correlations between nodal attributes in the disconnected networks and clinical metrics showed, in the executive control sub-network, a direct correlation between D and DF ($r=0.512$, $p<0.05$) and an inverse correlation between E and persistent errors at the WCST ($r=-0.599$, $p<0.05$) while, in the visual sub-network, a direct correlation between D and both Hoehn & Yahr stage ($r=0.545$, $p<0.05$) and UPDRS score ($r=0.548$, $p<0.05$) as well as an indirect correlation between E and incorrect answers/persistent errors at the

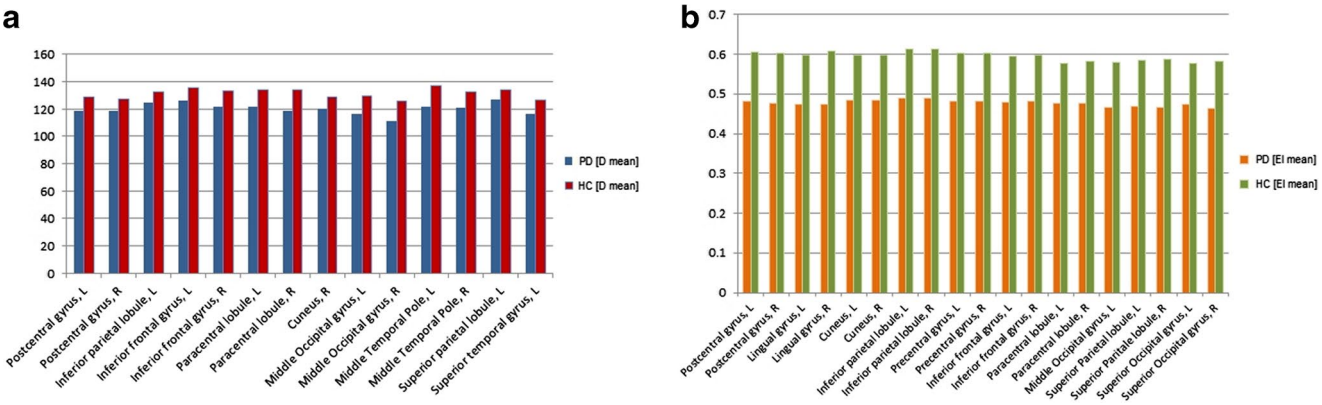

Fig. 2 D and E_l hubs. Statistically significant difference in degree hubs (**a**) and local efficiency hubs (**b**) in Parkinson's disease and healthy controls group ($p<0.05$)

Table 3 Hubs showing a significant lower local efficiency in PD than HC

Brain area	Coordinates			*p*-value
	x	y	z	
Postcentral gyrus, L	−40	−30	52	0.0170
Postcentral gyrus, R	46	−27	51	0.0157
Lingual gyrus, L	−8	−79	4	0.0121
Lingual gyrus, R	15	−75	4	0.0088 *
Cuneus, L	−11	97	9	0.0247
Cuneus, R	15	−90	12	0.0246
Inferior parietal lobule, L	−40	−34	46	0.0155
Inferior parietal lobule, R	34	−38	47	0.0169
Precentral gyrus, L	−46	−17	35	0.0175
Precentral gyrus, R	36	−33	48	0.0189
Inferior frontal gyrus, L	−48	8	31	0.0201
Inferior frontal gyrus, R	48	7	18	0.0190
Paracentral lobule, L	−7	−37	58	0.0340
Paracentral lobule, R	8	−35	57	0.0268
Middle occipital gyrus, L	−31	−76	12	0.0213
Superior parietal lobule. L	−18	−61	52	0.0130
Superior parietal lobule. R	19	−60	52	0.0108
Superior occipital gyrus, L	−16	−80	26	0.0300
Superior occipital gyrus, R	23	−77	27	0.0131

Hubs showing a statistically significant lower local efficiency in PD as compared to HC ($p<0.05$). The coordinates are given as stereotaxic coordinates referring to the atlas of Talairach and Tournoux

Abbreviations: L left, *R* right

*$p<0.01$

WCST (respectively $r=-0.618$, $p<0.05$ and $r=-0.792$, $p<0.01$) were present.

Regarding the global parameters, the C was higher in PD while L was lower, with the exception of sub-network 4, which includes connection between the basal ganglia and the occipital cortex.

Discussion

Our findings show, consistently with previous studies (Göttlich et al. 2013; Luo et al. 2015; Sang et al. 2015; Zhang et al. 2014), a preserved small-world network topology in PD but highlight the presence of a less efficient organization of the brain network, expressed by the presence of a lower clustering coefficient in comparison with healthy controls, in alignment with what described in other neurological and psychiatric diseases (Stam et al. 2009; van den Heuvel et al. 2013). The preservation of a small-world architecture in presence of pathology is not surprising, since essentially all real-world networks exhibit the high levels of local clustering and the short overall path length that characterize this organization. Rather, the distinctiveness of each network relies in the ways in which its small-world properties deviate from a randomly generated network, where all nodes have equal probability of being connected (Bullmore et al. 2009).

As a consequence, despite the small-world topology exhibited by PD patients, their small-world properties differ from the ones exhibited by the matched normal controls and reported in early-stage PD patients (Sang et al. 2015). Our population showed a lower local efficiency when compared with controls and no differences in terms of global efficiency, while, in early-stage PD patients, the converse has been generally found, with a significant decrease in

Table 4 Disconnected sub-networks in Parkinson's disease patients

Network index	Brain region	
1*	*Cerebellum IX Hem,L*	Anterior Cingulate Ctx, L
	Cerebellum IX Hem, R	Anterior Cingulate Ctx, L
2*	*Globus Pallidus Medial, R*	Inferior Frontal gyrus, L
	Globus Pallidus Medial, R	Supplementary Motor, L (area 6)
3**	*Globus Pallidus Lateral, L*	Supplementary Motor, L (area 4a)
	Cerebellum VII b, R	Intraparietal sulcus, L
	Globus Pallidus Lateral, L	Intraparietal sulcus, L
	Cerebellum VII b, R	Intraparietal sulcus, R
	Globus Pallidus Lateral, L	Inferior Temporal gyrus, L
	Globus Pallidus Lateral, L	Inferior Temporal gyrus, R
	Middle Temporal Pole, L	*Globus Pallidus Lateral, L*
4**	*Putamen, L*	Visual cortex, L (hOC5_V5)
	Middle Occipital gyrus, L	*Globus Pallidus Lateral, R*
	Putamen, L	*Middle Occipital gyrus, L*
	Putamen, L	*Middle Occipital gyrus, R*

The network index is used to group the region-pairs into a sub-network. Statistical significant differences are expressed as * for $p<0.05$ and ** for $p<0.01$

Abbreviations: L left, *R* right

global efficiency and without changes in local efficiency. Different PD stages seem therefore to exhibit different small-world patterns with a prevailing integration deficit in early PD and a prevalent segregation disruption in advanced PD.

Locally, patients with PD showed lower degree of connectivity in many hubs corresponding to functionally relevant areas involved in interpretation of sensory information and multimodal integrating functions. We confirm the presence of a decreased connectivity degree in the supplementary motor area, already described by Wu and colleagues and interpreted, considering the central role of this region in motor selection and initiation of movements, as a critical factor contributing to the development of akinesia in PD patients (Wu et al. 2009).

In addition, our findings revealed a decreased nodal degree in superior and inferior parietal lobule, whose crucial role in normal aging and neurodegenerative disorders has been reported by several fMRI studies (Delaveau et al. 2010; van Eimeren et al. 2009). A significantly lower degree in PD group was also detected in the inferior frontal gyrus, involved in suppression of habitual responses, an integral part of executive functions known to be affected in PD patients (Aarsland et al. 2012). These data, in addition to the overall lower local efficiency in PD patients compared to healthy controls, reflect diffuse, lower-level communication effectiveness between neighboring brain areas.

When we evaluated the inter regional functional connectivity, we identified four disconnected subnetworks in regions responsible for executive control, sensory-motor control and planning, motor coordination and visual elaboration. In particular, the disconnection of occipital cortex network in PD is consistent with a recent report (Tessitore et al. 2012). Since PD patients rely mainly on visual cues to

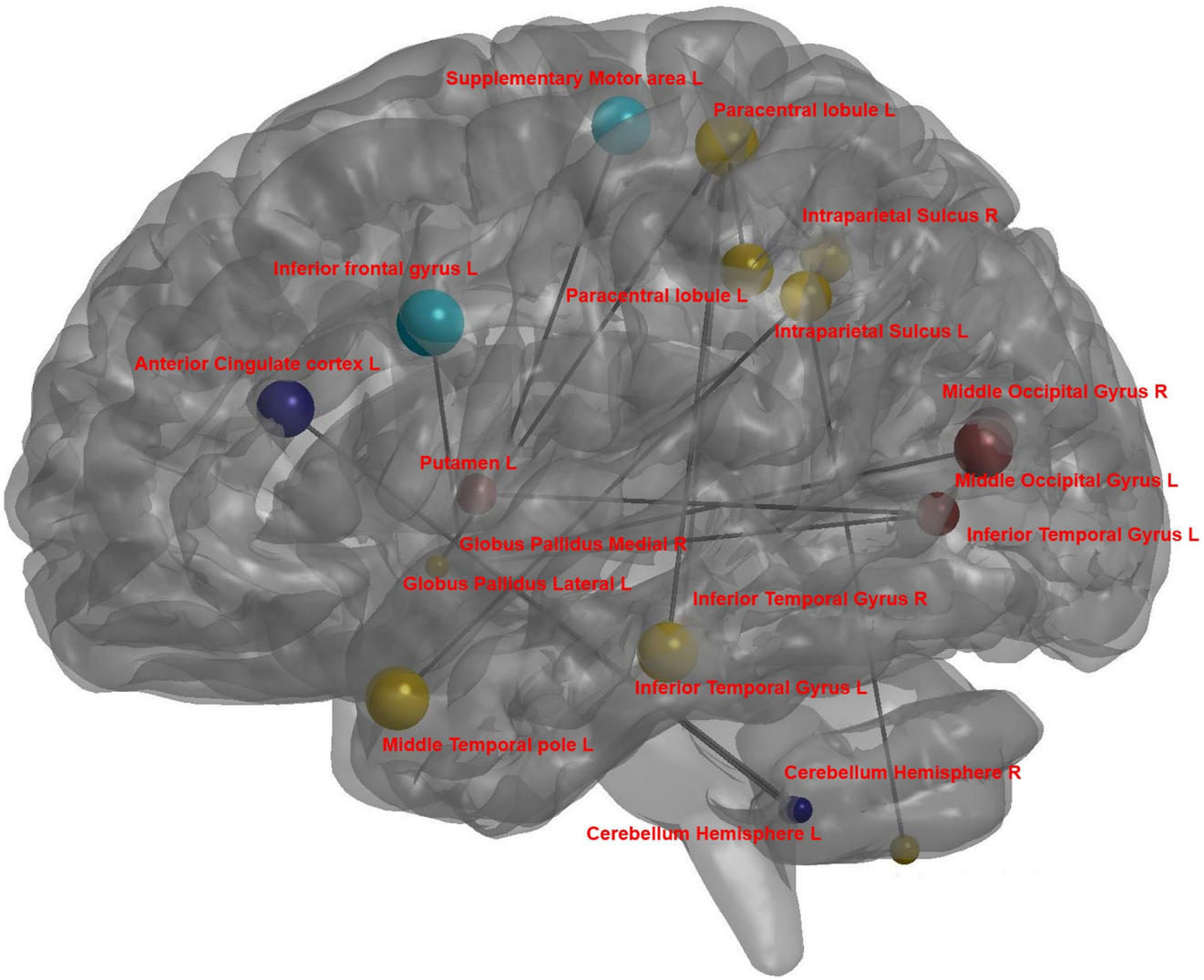

Fig. 3 Disconnected sub-networks in Parkinson's disease patients. Each sub-network is identified by a different color. The nodes dimension is proportional to the hubs degree. The links represent the statistically significant disconnected paths

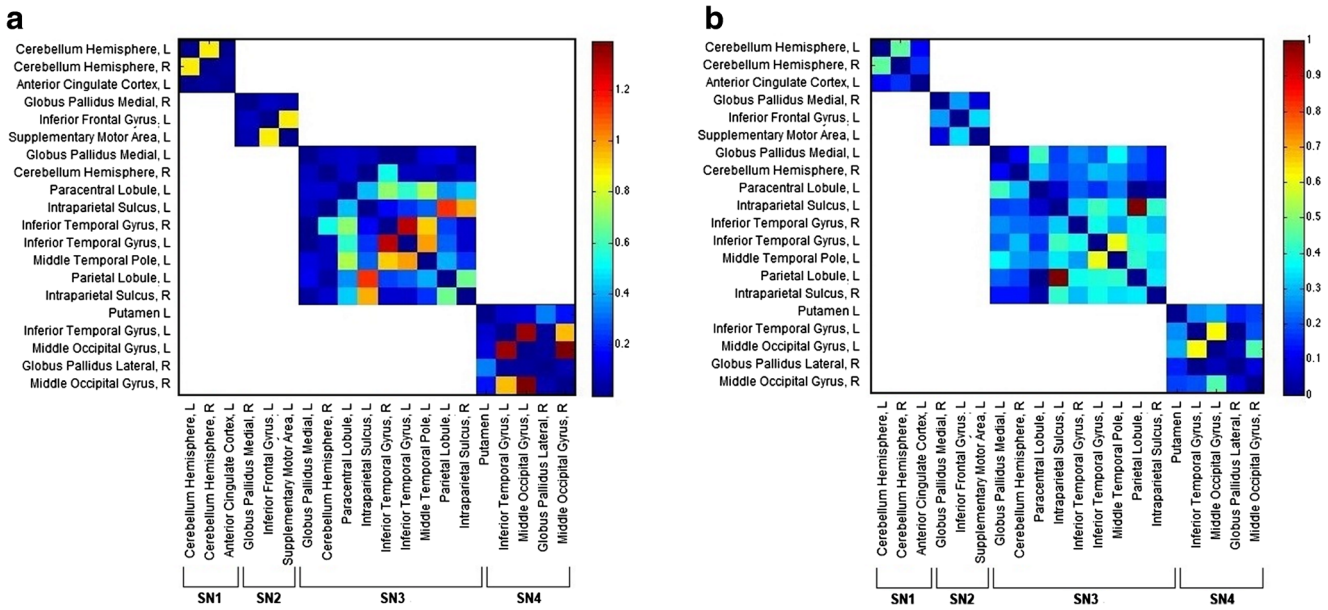

Fig. 4 Functional connectivity in altered subnetworks. Numbers from 1 to 4 identify the four disconnected sub-networks in Parkinson's disease (**a**) and healthy controls (**b**). Abbreviations: SN sub-networks

control locomotion (Sage and Almeida 2010), visual deficit have been correlated with gait disturbances and greater disability (Uc et al. 2005); moreover, the impairment of multimodal integration function of extrastriate cortex may contribute to the neuropsychological deficit in PD patients. Eventually, the disconnection of medial globus pallidus and cerebellum with areas involved in executive controls seems to mirror the pattern of cognitive impairment in PD with prevalent involvement of the fronto-subcortical attention-executive domain (Svenningsson et al. 2012). These hypothesis are further confirmed by the correlations we identified between nodal attributes of the disconnected networks and both motor and cognitive metrics.

The estimation of graph metrics within disconnected networks clarifies that not only they are poorly integrated in the global brain network but they also present increased fault susceptibility, as expressed by the lower local efficiency in comparison with healthy controls.

In contrast with previous reports (Lebedev et al. 2014; Vervoort et al. 2016; Wu et al. 2009), we did not identify any subnetwork showing enhanced connectivity. The lack of localized hyperconnectivity might be due to the down-regulation of functional connectivity induced by levodopa treatment (Wu et al. 2009). In alternative, it could be related to the longer disease duration and more advanced disease stage of our population, which could explain a decline in compensatory connectivity over time.

Although no correlations were identified between graph parameters and LEDD, the lack of correlations between most of our functional metrics and motor scores could still be attributed to the potentially confounding effects of chronic dopaminergic medications, that can partially restore the deficits in the functional brain network (Delaveau et al. 2010).

With regard to the clinical impact of our findings, we detected a significant direct correlation between the DSS scores, expression of information processing speed, and the degree of connectivity of the superior frontal gyrus, responsible for manipulation of relevant information and

Table 5 Graph parameters in disconnected sub-networks

Network	Metric	Parkinson's disease	Healthy controls	*p*-value
1	D	87.550 ± 23.720	84.45 ± 24.592	0.397
	E_l	0.398 ± 0.067	0.412 ± 0.103	0.538
	C	0.015 ± 0.009	0.052 ± 0.014	**< 0.01**
	L	0.726 ± 0.278	0.791 ± 0.269	**< 0.05**
2	D	101.817 ± 30.279	106.358 ± 32.149	0.062
	E_l	0.387 ± 0.128	0.473 ± 0.181	**< 0.05**
	C	0.026 ± 0.011	0.051 ± 0.019	**< 0.01**
	L	0.792 ± 0.269	0.985 ± 0.049	**< 0.01**
3	D	105.319 ± 23.323	114.078 ± 23.601	**< 0.01**
	E_l	0.414 ± 0.102	0.520 ± 0.150	**< 0.01**
	C	0.307 ± 0.054	0.398 ± 0.086	**< 0.01**
	L	0.820 ± 0.202	0.830 ± 0.206	0.621
4	D	96.881 ± 21.702	109.483 ± 21.975	**< 0.01**
	E_l	0.385 ± 0.119	0.506 ± 0.164	**< 0.01**
	C	0.278 ± 0.058	0.166 ± 0	**< 0.01**
	L	0.820 ± 0.267	0.78 ± 0.205	**< 0.01**

Graph theory measures with significant statistical differences in Parkinson's disease compared with healthy controls are in bold

Abbreviations: D degree of connectivity, E_l local efficiency, *C* clustering coefficient, *L* path length

subsequent organization of sequence of actions. DSS score was also directly correlated with local efficiency in areas involved in inhibiting behavior, motor planning and visual association. WCST score, a measure of executive functions, was directly correlated with E_l of areas involved in sensory and visual perception, integration and elaboration of sensory inputs and motor execution.

Although our findings are preliminary, we speculate that, in a context of reduced network segregation, the presence of higher local efficiency in hubs regions correlates with a better cognitive performance. The lack of neuropsychological data in our control population prevented us from drawing conclusions on the pathological specificity of our results.

The main limitation of the present study is the small sample size. In particular, having only four patients with a tremor-dominant subtype, we could not investigate differences in brain networks in relation to the clinical phenotype; larger studies could provide more information about the neural bases of tremor-dominant vs akinetic-rigid phenotype.

In addition, even if our choice of analyzing PD patients under chronic antiparkinsonian treatment reflects accurately a real-world population, it might have added confounding factors to the results interpretation. Although the chronic use of dopaminergic therapy influences cerebral networks and cortical plasticity, withdrawal from dopaminergic medication would have not been sufficient to reverse such effects and would have caused practical difficulties. Further studies in drug-naïve patients, are warranted to define the acute effects of dopaminergic drugs.

Finally, in the light of recent findings on diffusion-based structural connectivity in PD (Galantucci et al. 2017; Nigro et al. 2016), the integration of structural and functional data might, in the future, help elucidate the basis of the functional plasticity observed in PD and its clinical impact on patients' cognitive status.

In conclusion, we investigated for the first time the functional abnormalities responsible for motor and cognitive deficits in mid-stage PD patients under chronic antiparkinson treatment. Although further studies on larger cohorts are needed to confirm this hypothesis, our results suggest that, while functional reorganization appears in both motor and cognitive areas, the clinical expression of network imbalance seems to be partially compensated by the chronic levodopa treatment with regards to the motor but not to the cognitive performance.

Acknowledgements This work was supported by a grant from McDonnell Foundation (MFG), NIH R01 NS054864 (MFG), a large grant from NPF (MFG, ADR) and research funds from the Noto Foundation (MI) and Fondazione Italiana Sclerosi Multipla (MP).

Compliance with ethical standards

Financial disclosure Dr. Roxana Vancea has nothing to disclose.

Dr. Kristina Simonyan was supported by the National Institute on Deafness and Other Communication Disorders and National Institute of Neurological Disorders and Stroke, National Institutes of Health (R01DC011805, R01DC0123545, R01NS088160). Dr. Kristina Simonyan is a current member of the medical and scientific advisory council of the Dystonia Medical Research Foundation.
Dr. Maria Petracca has nothing to disclose.
Dr. Miroslaw Brys is currently an employee of Biogen and receives salary and stocks from the company.
Dr. Alessandro Di Rocco has nothing to disclose.
Dr. Maria Felice Ghilardi has nothing to disclose.
Dr. Matilde Inglese has received research grants from NIH, NMSS, Novartis Pharmaceuticals Corp, Teva Neuroscience.

Informed consent The study was approved by the NYULMC Internal Review Board and all the subjects gave informed written consent prior to participation.

Ethical approval All procedures performed in studies involving human participants were in accordance with the ethical standards of the institutional and/or national research committee and with the 1964 Helsinki declaration and its later amendments or comparable ethical standards.

References

Aarsland, D., Brønnick, K., & Larsen, J. P. (2012). Cognitive impairment in incident, untreated Parkinson disease: the Norwegian ParkWest study. *Neurology, 72*, 1121–1126. https://doi.org/10.1212/01.wnl.0000338632.00552.cb.

Bassett, D. S., & Bullmore, E. (2006). Small-world brain networks. *The Neuroscientist, 12*(6), 512–523. https://doi.org/10.1177/1073858406293182.

Bullmore, E. T., Sporns, O., & Solla, S. A. (2009). Complex brain networks: graph theoretical analysis of structural and functional systems. *Nature Reviews. Neuroscience, 10*(3), 186–198. https://doi.org/10.1038/nrn2575.

Delaveau, P., Salgado-Pineda, P., Fossati, P., Witjas, T., Azulay, J. P., & Blin, O. (2010). Dopaminergic modulation of the default mode network in Parkinson's disease. *European Neuropsychopharmacology, 20*(11), 784–792. https://doi.org/10.1016/j.euroneuro.2010.07.001.

Esposito, F., Tessitore, A., Giordano, A., De Micco, R., Paccone, A., Conforti, R., et al. (2013). Rhythm-specific modulation of the sensorimotor network in drug-naive patients with Parkinson's disease by levodopa. *Brain: a Journal of Neurology, 136*(3), 710–725. https://doi.org/10.1093/brain/awt007.

Galantucci, S., Agosta, F., Stefanova, E., Basaia, S., van den Heuvel, M. P., Stojkovic, T., et al. (2017). Structural brain connectome and cognitive impairment in Parkinson disease. *Radiology, 283*(2), 515–525.

Goetz, C. G., Fahn, S., Martinez-Martin, P., Poewe, W., Sampaio, C., Stebbins, G. T., et al. (2007). Movement disorder society-sponsored revision of the unified Parkinson's disease rating scale (MDS-UPDRS): process, format, and clinimetric testing plan. *Movement Disorders, 22*(1), 41–47. https://doi.org/10.1002/mds.21198.

Göttlich, M., Münte, T. F., Heldmann, M., Kasten, M., Hagenah, J., & Krämer, U. M. (2013). Altered resting state brain networks in Parkinson's disease. *PLoS ONE, 8*(10), e77336. https://doi.org/10.1371/journal.pone.0077336.

Hughes, A. J., Daniel, S. E., Kilford, L., & Lees, A. J. (1992). Accuracy of clinical diagnosis of idiopathic Parkinson's disease: a clinico-pathological study of 100 cases. *Journal of Neurology,*

Neurosurgery & Psychiatry, 55, 181–184. https://doi.org/10.1136/jnnp.55.3.181.

Lebedev, A. V., Westman, E., Simmons, A., Lebedeva, A., Siepel, F. J., Pereira, J. B., & Aarsland, D. (2014). Large-scale resting state network correlates of cognitive impairment in Parkinson's disease and related dopaminergic deficits. *Frontiers in Systems Neuroscience, 8*(4), 45. https://doi.org/10.3389/fnsys.2014.00045.

Luo, C., Song, W., Chen, Q., Zheng, Z., Chen, K., Cao, B., et al. (2014). Reduced functional connectivity in early-stage drug-naive Parkinson's disease: a resting-state fMRI study. *Neurobiology of Aging, 35*(2), 431–441. https://doi.org/10.1016/j.neurobiolaging.2013.08.018.

Luo, C. Y., Guo, X. Y., Song, W., Chen, Q., Cao, B., Yang, J., et al. (2015). Functional connectome assessed using graph theory in drug-naive Parkinson's disease. *Journal of Neurology, 262*(6), 1557–1567. https://doi.org/10.1007/s00415-015-7750-3.

Matsumoto, M. (2015). Dopamine signals and physiological origin of cognitive dysfunction in Parkinson's disease. *Movement Disorders, 30*(4), 472–483. https://doi.org/10.1002/mds.26177.

Mattis, P. J., Tang, C. C., Ma, Y., Dhawan, V., & Eidelberg, D. (2011). Network correlates of the cognitive response to levodopa in Parkinson disease. *Neurology, 77*(9), 858–865. https://doi.org/10.1212/WNL.0b013e31822c6224.

Nigro, S., Riccelli, R., Passamonti, L., Arabia, G., Morelli, M., Nistico, R., et al. (2016). Characterizing structural neural networks in de novo Parkinson disease patients using diffusion tensor imaging. *Human Brain Mapping, 37*(12), 4500–4510. https://doi.org/10.1002/hbm.23324.

Poletti, M., & Bonuccelli, U. (2013). Acute and chronic cognitive effects of levodopa and dopamine agonists on patients with Parkinson's disease: a review. *Therapeutic Advances in Psychopharmacology, 3*(2), 101–113. https://doi.org/10.1177/2045125312470130.

Reijmer, Y. D., Leemans, A., Caeyenberghs, K., Heringa, S. M., Koek, H. L., & Biessels, G. J. (2013). Disruption of cerebral networks and cognitive impairment in Alzheimer disease. *Neurology, 80*(15), 1370–1377.

Rubinov, M., & Sporns, O. (2010). Complex network measures of brain connectivity: uses and interpretations. *NeuroImage, 52*(3), 1059–1069. https://doi.org/10.1016/j.neuroimage.2009.10.003.

Sage, M. D., & Almeida, Q. J. (2010). A positive influence of vision on motor symptoms during sensory attention focused exercise for Parkinson's disease. *Movement Disorders, 25*(1), 64–69. https://doi.org/10.1002/mds.22886.

Sang, L., Zhang, J., Wang, L., Zhang, J., Zhang, Y., Li, P., et al. (2015). Alteration of brain functional networks in early-stage Parkinson's disease: a resting-state fMRI study. *Plos One, 10*(10), e0141815. https://doi.org/10.1371/journal.pone.0141815.

Skidmore, F., Korenkevych, D., Liu, Y., He, G., Bullmore, E., & Pardalos, P. M. (2011). Connectivity brain networks based on wavelet correlation analysis in Parkinson fMRI data. *Neuroscience Letters, 499*(1), 47–51. https://doi.org/10.1016/j.neulet.2011.05.030.

Stam, C. J., De Haan, W., Daffertshofer, A., Jones, B. F., Manshanden, I., Van Cappellen Van Walsum, A. M., et al. (2009). Graph theoretical analysis of magnetoencephalographic functional connectivity in Alzheimer's disease. *Brain: a Journal of Neurology, 132*(1), 213–224. https://doi.org/10.1093/brain/awn262.

Svenningsson, P., Westman, E., Ballard, C., & Aarsland, D. (2012). Cognitive impairment in patients with Parkinson's disease: diagnosis, biomarkers, and treatment. *The Lancet Neurology, 11*(8), 697–707. https://doi.org/10.1016/S1474-4422(12)70152-7.

Tessitore, A., Esposito, F., Vitale, C., Santangelo, G., Amboni, M., Russo, A., Corbo, D., Cirillo, G., Barone, P., Tedeschi, G. (2012). Default-mode network connectivity in cognitively unimpaired patients with Parkinson disease. *Neurology, 79*(23), 2226–2232. https://doi.org/10.1212/01.wnl.0000436943.62904.09.

Uc, E. Y., Rizzo, M., Anderson, S. W., Qian, S., Rodnitzky, R. L., & Dawson, J. D. (2005). Visual dysfunction in Parkinson disease without dementia. *Neurology, 65*(12), 1907–1913. https://doi.org/10.1212/01.wnl.0000191565.11065.11.

van den Heuvel, M. P., Sporns, O., Collin, G., Scheewe, T., Mandl, R. C. W., Cahn, W., et al. (2013). Abnormal rich club organization and functional brain dynamics in schizophrenia. *JAMA Psychiatry, 70*(8), 783–792. https://doi.org/10.1001/jamapsychiatry.2013.1328.

van Eimeren, T., Monchi, O., Ballanger, B., & Strafella, A. (2009). Dysfunction of the default mode network in Parkinson disease: a functional magnetic resonance imaging study. *Archives of Neurology, 66*(7), 877–883. https://doi.org/10.1001/jamaneurol.2013.5528.

Vervoort, G., Alaerts, K., Bengevoord, A., Nackaerts, E., Heremans, E., Vandenberghe, W., & Nieuwboer, A. (2016). Functional connectivity alterations in the motor and fronto-parietal network relate to behavioral heterogeneity in Parkinson's disease. *Parkinsonism & Related Disorders, 24*, 48–55. https://doi.org/10.1016/j.parkreldis.2016.01.016.

Worbe, Y., Malherbe, C., Hartmann, A., Pelegrini-Issac, M., Messe, A., Vidailhet, M., et al. (2012). Functional immaturity of cortico-basal ganglia networks in Gilles de la Tourette syndrome. *Brain: a Journal of Neurology, 135*(6), 1937–1946. https://doi.org/10.1093/brain/aws056.

Wu, T., Wang, L., Chen, Y., Zhao, C., Li, K., & Chan, P. (2009). Changes of functional connectivity of the motor network in the resting state in Parkinson's disease. *Neuroscience Letters, 460*(1), 6–10. https://doi.org/10.1016/j.neulet.2009.05.046.

Zalesky, A., Fornito, A., & Bullmore, E. T. (2010). Network-based statistic: identifying differences in brain networks. *NeuroImage, 53*(4), 1197–1207. https://doi.org/10.1016/j.neuroimage.2010.06.041.

Zhang, D., Liu, X., Chen, J., Liu, B., & Chan, C. (2014). Distinguishing patients with Parkinson's disease subtypes from normal controls based on functional network regional efficiencies. *PLoS ONE, 9*(12), 1–18. https://doi.org/10.1371/journal.pone.0115131.